



PERGAMON

Journal of Quantitative Spectroscopy &
Radiative Transfer 83 (2004) 655–666

Journal of
Quantitative
Spectroscopy &
Radiative
Transfer

www.elsevier.com/locate/jqsrt

Passive remote detection in a combustion system with a tunable heterodyne receiver: application to sulfur dioxide

D. Weidmann*, D. Courtois

Groupe de Spectroscopie Moléculaire et Atmosphérique, Faculté des Sciences Exactes et Naturelles, Université de Reims Champagne-Ardenne, UMR CNRS 6089, BP 1039, 51687 REIMS Cedex 2, France

Received 25 September 2002; accepted 27 February 2003

Abstract

Here is presented the possibility of remote detection of sulfur dioxide in a combustion chamber. It is of major interest as part of the program of global pollution reduction. The remote detection of combustion products in the middle infrared region can be very useful for engine diagnostics or industrial pollution control.

We used a tunable diode laser heterodyne receiver working in the middle infrared. Such an apparatus is able to perform passive emission spectroscopy on distant sources. It is a very sensitive and selective technique for radiation detection able to extract weak signals from the background. To validate our prototype and demonstrate its efficiency, we recorded high-temperature sulfur dioxide emission spectra around 1336 cm^{-1} (ν_3 ro-vibrational band), in the case of a polluted CH_4/air flame.

© 2003 Elsevier Ltd. All rights reserved.

Keywords: Diode laser; Heterodyne spectroscopy; Middle infrared; Optical remote sensing; Sulfur dioxide; Combustion diagnostics

1. Introduction

The remote detection of atmospheric pollutants has become a very important issue and reducing polluting emissions involves their monitoring. Some of the atmospheric pollutants are often generated by combustion of fossil fuels, the major source of energy exploited by industrial countries. The monitoring technique to use depends on measurement conditions.

A large panel of diagnostic methods, using spectroscopic tools and lasers, are available. Techniques like laser induced grating (LIG) [1–3], laser induced fluorescence (LIF) [4], coherent anti-stokes

* Corresponding author. Present address: Rice University MS366, ECE Dept., 6100 Main Street, Houston, TX 77251-1832, USA. Tel.: 1-713-348-3508; fax: 1-713-348-5686.

E-mail address: weidmann@rice.edu (D. Weidmann).

Raman scattering (CARS) [5–7], and tunable diode laser absorption spectroscopy (TDLS) [8–11] are widely used as far as only in situ measurements are considered. But, for long-range remote sensing, only differential absorption lidar (DIAL) [12–14] and radiometers are suitable instruments.

DIAL can suffer from two drawbacks, depending on the application: it is an active way of sensing and as a consequence does not provide discretion, and it has a limited operating range, at best 5 km for conventional lidar [15].

In comparison, infrared radiometers are passive remote-sensing instruments and are not limited in range. Most of the molecules presents a non-ambiguous signature in the middle infrared region of the electromagnetic spectrum, corresponding to ro-vibrational transitions and falling into the 8–12 μm atmospheric window. Collecting emission spectra at these wavelengths can provide pertinent qualitative and quantitative information about a distant radiative source. The source radiation can be collected in a direct detection scheme and analyzed by a Fourier Transform Spectrometer [16]. However, when high sensitivity and high spectral resolution are both needed, heterodyne receivers are the most pertinent instruments to perform radiometry [17]. This kind of instrument is particularly suitable as far as sources to detect are very distant or very small.

The emergence of Quantum Cascade Lasers [18], which will be able to provide room temperature, good-quality infrared tunable local oscillators, must boost the interest in tunable heterodyne receivers.

In a previous paper [19], we took under consideration the use of heterodyne radiometry in combustion detection. We demonstrated that a tunable diode laser middle infrared heterodyne radiometer is relevant in detecting water vapor at high-temperature emission lines, and this, in spite of a low-power lead salt semiconductor laser as tunable local oscillator. This demonstration would find promising applications in detecting thrust nozzles exhaust gases.

In this paper, we will still consider tunable heterodyne radiometry in a combustion process. But now, we will focus on the detection of sulfur dioxide, as it is a major combustion pollutant. But unlike water vapor, it has a very low emissivity at high temperature.

In the first section, we will deal with heterodyne radiometry and the instrument will be presented.

In Section 2, we will consider the particular case of SO_2 as middle infrared thermal emitter. We will see that high-temperature sulfur dioxide presents a low-emission coefficient in the 7–10 μm range.

The last section will present a typical SO_2 emission spectrum proving the instrument efficiency and some ways of improvements will be indicated.

2. Heterodyne radiometry

2.1. Principle of operation

Using the heterodyne detection technique permits to detect middle infrared electromagnetic radiation emitted by a distant source in an analysis bandwidth B centered at the local oscillator frequency. B is defined by an ordinary radio frequency (RF) passive filter or by the photomixer electrical bandwidth. Since we use a tunable local oscillator, the radiometer can be converted to a passive emission spectrometer.

The structure of the radiometer is sketched in Fig. 1. It is similar to a Dicke radiometer usually used in radio astronomy [20]. Let us comment on it.

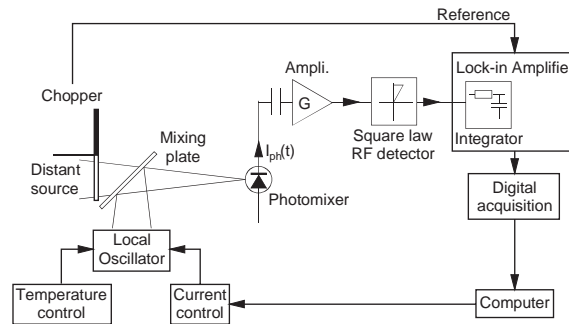


Fig. 1. Diagram of the radiometer setup. In this case, the analysis bandwidth of the heterodyne radiometer is defined by the photomixer bandwidth.

The thermal radiation coming from a distant phase gas molecular specie (the source) is mixed with the local oscillator beam onto a high-speed photomixer by a mixing plate. The quadratic detection then provides a photocurrent whose power spectrum is the frequency transposition, in the RF domain, of a part of the source spectrum [21]. Signals are then amplified. The RF power included in the photomixer bandwidth (when no RF filter is used) is detected by an RF quadratic detector. To discriminate the signal from the local oscillator shot noise, the source beam is amplitude modulated, then, a lock-in amplifier is used to demodulate signal of interest. As a consequence, this kind of system is able to measure a signal proportional to the power radiated by the optical source in the B band centered on the local oscillator frequency.

2.2. Tunable lead salt lasers as local oscillator

Using a tunable local oscillator (LO) permits to tune the analyzed source spectrum zone. If B is smaller than the source spectral structure width, by tuning the LO frequency, we can record simultaneously an exact image of the source spectrum (see Fig. 2).

In the middle infrared region, double heterostructure lead salt diode lasers (DL) provide a widely tunable laser [22]. Typically, such a laser exhibits $1\text{--}2\text{ cm}^{-1}$ continuously tunable zones separated by $4\text{--}5\text{ cm}^{-1}$ discrete mode hops depending on laser cavity length. In this work we use this kind of bipolar semiconductor lasers as local oscillator emitting around $7.5\text{ }\mu\text{m}$.

As LO, lead salt DLs suffer from drawback of multimode emission at high optical power. Indeed, in heterodyne detection a natural single mode laser is required, otherwise excess noise introduced by the LO totally screens the heterodyne signal. This problem was treated, for example, by Katzberg et al. [23]. DLs are often single mode only near the threshold. As a consequence, the optical power available is low and the heterodyne receiver operates far from ideal conditions [24].

2.3. Signal-to-noise ratio

A treatment of heterodyne systems signal-to-noise ratio (SNR) can be found in the literature [25–28]. To take into account the excess noise and the low power LO, the post-detection general SNR

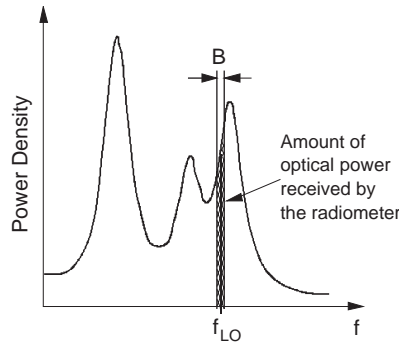


Fig. 2. Sketch of the source spectrum, where is schematized the analysis bandwidth B centered on the LO frequency. By tuning the LO frequency, an almost exact image of the source spectrum can be recorded, subject to B is smaller than the typical widths of the source spectrum structures.

can be written as

$$SNR = \frac{(\eta e/hf)^2 P_{LO} P_S \sqrt{B\tau}}{e(\eta e/hf)(P_{OL} + P_B + P_{ex})B + 2kB(T_a/R_a)}, \tag{1}$$

with η being photomixer quantum efficiency, f the optical frequency, and P_{LO}, P_S, P_B, P_{ex} as the LO power, the source power, the background power and the excess noise equivalent power, respectively; T_a and R_a are the amplifier noise temperature and the amplifier input impedance, respectively, and τ is the integrator time constant.

In the particular case of a radiometer, under the assumption that the analysis bandwidth is small compared to the structure width of the source spectrum, the source power, coming from a homogeneous phase gas molecular species and received by the instrument is

$$P_s = \varepsilon(f)L_f^0(T_S)\lambda^2 B, \tag{2}$$

where λ^2 is the coherent étendue T_S the gas temperature, and $\varepsilon(f)$ the gas emissivity containing spectral information.

2.4. SO₂ as thermal emitter

SO₂ is a widespread industrial pollutant. It appears during the combustion of oils or hydrocarbons containing residual amounts of sulfur. The exothermic nature of combustion involves the generation of high-temperature sulfur dioxide. We will see that this gas is difficult to detect by a radiometer even at combustion temperature.

In the middle infrared, the strongest SO₂ ro-vibrational band is the ν_3 band centered at 1362 cm⁻¹. Fig. 3 shows ν_3 band transition intensities for 296 and 1500 K. Data are taken from Hitran96 database [29].

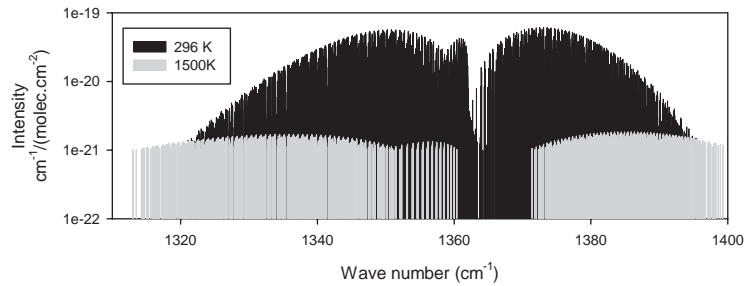


Fig. 3. ν_3 band SO_2 transition intensities for 296 and 1500 K.

At 1500 K, due to the level occupation statistic, transition intensities collapse. As a result, sulfur dioxide emissivity becomes very low.

But emissivity is not the only parameter to take into account. Planck luminance appears in the Eq. (2), so the source temperature is involved too.

We computed the amount of power radiated by SO_2 . The source parameters chosen are: 5 Torr of SO_2 mixed with 100 Torr of air, a medium of 2 cm length, and a spectral region around 1335.8 cm^{-1} corresponding to the ν_3 band. These parameters are coarse near our experimental conditions, which will be seen in the next section.

Fig. 4 is the source blackbody equivalent temperature versus the wavenumber. On this graph we present four different source temperatures. Fig. 5 presents the source blackbody equivalent temperature versus the actual source temperature, for a given frequency corresponding to the top of Fig. 4 first emission line. With this analysis, it appears that, for sulfur dioxide, increasing the temperature does not necessarily increase the amount of optical power radiated, since ro-vibrational transition intensities strongly decrease. A maximum emission exists around 900 K, in the case presented here.

Sulfur dioxide appears to be a bad emitter at high temperatures. To detect it by radiometry, high sensivity is necessary. A heterodyne radiometer thus seems to be pertinent.

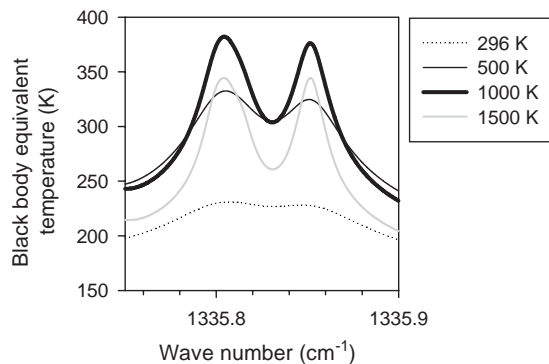


Fig. 4. Calculation of blackbody equivalent temperature of a 2 cm length mixture containing 5 Torr of SO_2 and 100 Torr of air versus wavenumber, for four different SO_2 actual temperatures.

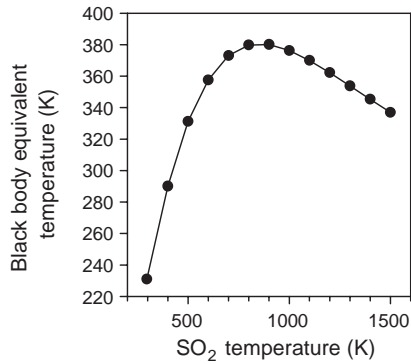


Fig. 5. Source blackbody equivalent temperature versus actual source temperature, at a fixed frequency corresponding to the top of the first line appearing in Fig. 4. At high temperature, the decrease of transition intensities involves a decrease of power radiated by SO₂.

3. Experiment and results

3.1. Heterodyne radiometer setup

The optical setup of our radiometer has already been described in a previous paper [19]. Fig. 6 shows a sketch of the setup. The DL is mounted inside a high stability cryostat designed at the laboratory [30]. The beam coming from the LO is mixed with radiation coming from a flat flame burner also designed at the laboratory [31], onto a high speed HgCdTe photomixer. As sketched

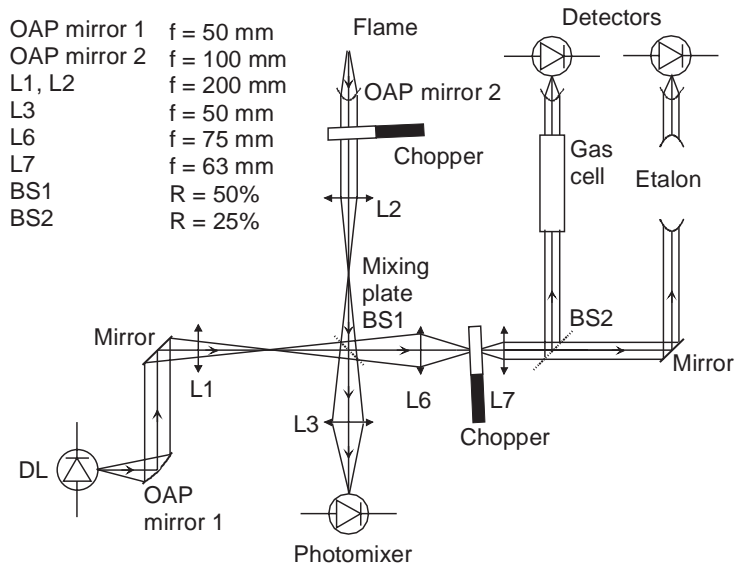


Fig. 6. Diagram of the optical setup.

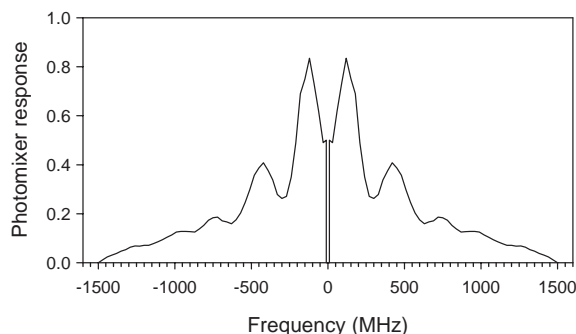


Fig. 7. Photomixer frequency response, the effective analysis bandwidth of the radiometer is about 700 MHz.

in Fig. 1, the RF signal is then amplified and detected. A lock-in amplifier demodulates the signal before the digital acquisition. The acquisition is synchronized with the current source, which tunes the LO.

As any RF filter is used between amplifiers and RF detector, the radiometer analysis bandwidth is the effective electrical bandwidth of the photomixer. Moreover, the photomixer frequency response makes up the radiometer apparatus function. The original source emission spectrum will be convolved by this function, appearing in Fig. 7.

3.2. Source: flat flame burner

To be close to realistic combustion conditions, we designed a specific burner as source to validate our tunable heterodyne radiometer prototype. As it remains a prototype working in the laboratory, the range of detection is short: the combustion chamber is nearby the optical antenna.

The system was already described [31]. It produces a low-pressure CH₄/air premixed flame. To create a polluting flame, we added to the fuel/oxidant mixture a small amount of sulfur dioxide. In the burned gas region of the flame, the SO₂ is heated to a high temperature (around 1300 K), and the radiation coming from this region is collected by the optical antenna of the heterodyne radiometer.

3.3. LO frequency calibration

The LO frequency must hit the ro-vibrational transition lines of the molecular species to probe. For this purpose, a fine LO frequency calibration is needed. Here, we perform it by tunable diode laser absorption spectroscopy. The part of the diode laser radiation, which is not used for illuminating the photomixer goes both through a reference gas cell and through a confocal Fabry–Pérot etalon.

A relative frequency calibration is given by the etalon; the free spectral range is of 0.01 cm⁻¹. As it is a high finesse etalon [32], the fringe sight gives us information on the diode laser emission linewidth.

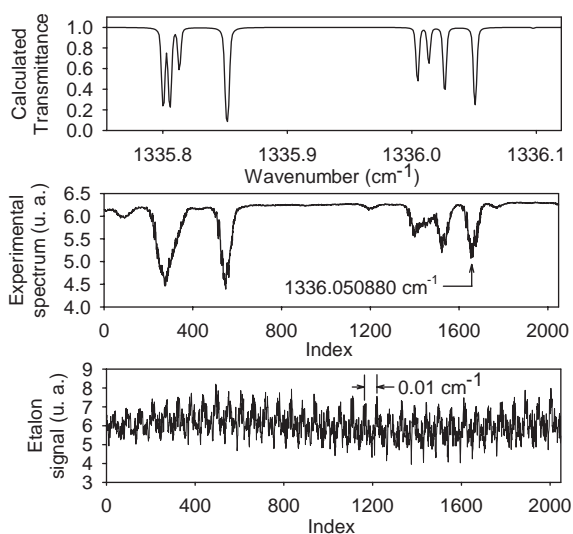


Fig. 8. Typical LO frequency calibration spectrum obtained by tunable diode laser absorption spectroscopy. The above graph is the calculated spectra used for absolute frequency calibration. The graph on the middle is the experimental SO_2 spectrum (20 cm, 0.5 Torr). The graph below is the signal provided by the confocal Fabry–Pérot etalon given the relative frequency calibration. One can note an important degradation of the finesse due to a lack of diode laser injection current stability.

The absolute frequency calibration is given by the 20-cm-length reference absorption cell, typically filled with 0.5 Torr of SO_2 . The absolute frequency is deduced by comparison with calculated spectra based on Hitran96 data.

Fig. 8 shows the typical calibration signals recorded. They present the continuous tunable spectral zone chosen for the LO.

Once the calibration is done, the current ramp, the current setpoint and the temperature setpoint to be applied to the diode laser are known. We then record heterodyne emission spectra under these conditions.

4. Results: emission spectra of SO_2

Fig. 9 presents the SO_2 emission spectrum recorded by heterodyne tunable radiometry under the experimental conditions summarized in Table 1. The LO power remains one-third below the 300 μW power required for good operation [24]. The analysis bandwidth is adapted to the linewidth of SO_2 lines, which are collision broadened due to the chamber pressure. On the figure appears, in solid line, the calculated flux received by the radiometer. This calculation was made with a simple radiative transfers model described in [19] and takes into account the apparatus function appearing in Fig. 6.

The spectrum of Fig. 9 proves that, in spite of a very low sulfur dioxide emissivity and a low-power LO, the tunable heterodyne receivers can provide an emission spectrum. Such a spectrum is a non-ambiguous signature of the molecule and allows identification. In addition, quantitative

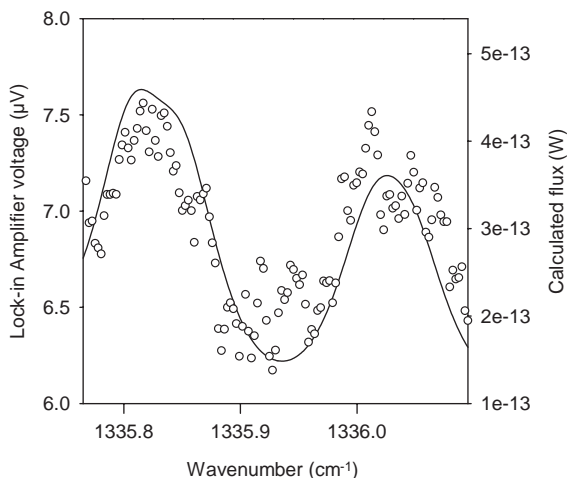


Fig. 9. Experimental (dots) and calculated (solid line) heterodyne emission spectra of 5 Torr of SO₂ polluting a 175 Torr CH₄/air premixed flame.

Table 1

Experimental conditions corresponding to the spectrum appearing in Fig. 8

LO temperature	92.6 K
LO current	1000 mA
LO current ramp spread	14 mA
LO optical power	120 μW
Effective analysis bandwidth	700 MHz
Integration time	3 s
Total recording time	26 min
Flame pressure	175 Torr
SO ₂ partial pressure	5 Torr

information on concentration and/or temperature can be deduced by using least-squares fitting algorithms, and thus allows remote monitoring.

5. Ways of improvement

From the spectrum of Fig. 9, a reliable detection limit can be estimated to be 2×10^{-13} W, the theoretical shot noise limited detection limit would be 100 times lower, but low-power LO and excess noise degrades the instrument sensitivity, as indicated by Eq. (1).

The experimental limit is easily improvable by using a more powerful LO. But what are kinds of tunable mid-infrared laser sources, emitting in the 8–12 μm atmospheric window, available? Several tracks of semiconductor lasers seem to be promising for the future:

- *Lead salt multi-quantum well lasers* [33]. By now, they emit around 6.1 μm in CW mode at 210 K, but an optical pumping provided by an Nd: YAG is necessary.

Table 2

Calculation of the minimum detectable concentration of several molecules, considering a 1 m length medium at 2000 K, and a heterodyne receiver with 2×10^{-15} W as minimum detectable power (shot noise limited)

Molec.	Transition frequency (cm^{-1})	Intensity at 2000 K $\text{cm}^{-1}(\text{molec. cm}^{-2})$	Detectable concentration in 750 Torr of air
H ₂ O	1205.104353	1.061×10^{-21}	4 ppm
CO ₂	0942.874488	1.023×10^{-21}	20 ppm
SO ₂	1328.92977	6.075×10^{-22}	20 ppm
N ₂ O	1241.58920	1.754×10^{-21}	5 ppm
H ₂ S	1315.538820	8.597×10^{-23}	200 ppm
NO ₂	1250.135284	1.414×10^{-23}	0.6%

- *Vertical cavity surface emitting lasers* [34]. At the present, they emit around 4.5 μm , at 290 K, but only in the pulsed mode.
- *Interband cascade lasers* [35]. They emit around 3.9 μm , at 217 K, in the pulsed mode.
- *Quantum cascade lasers* [36]. They now emit around 9.1 μm , at room temperature, and in the CW mode.

Among the four kinds of lasers listed above, the first three are not yet ready to be used as heterodyne tunable local oscillator. Some more developments are needed. In return, distributed feedback quantum cascade lasers are now proved to be a suitable mid-IR LO, since high single mode power is available. With such a laser, we experimentally observed a 3 cm^{-1} continuously tunable single-mode zone at power of several mW with excellent spectral purity at liquid nitrogen temperature. These tunable laser components would take part in the development of light, transportable, passive remote sensing instruments like heterodyne receivers.

If we suppose that the detection limit of our heterodyne receiver is increased by a factor 100, to reach the shot noise limited value 2×10^{-15} W, thanks to quality-improved LO, let us see, for several molecules, the detectable concentration in atmospheric air, in the 8–12 μm window.

For this estimation, we considered a homogeneous medium at 2000 K and of 1 m length with a sky background. The results are indicated in Table 2. Note that CO is poor thermal emitter at these wavelengths to be detected in low concentration.

Let us collect that the concentration appearing in Table 2 are passively remote measured.

6. Conclusion

This work aimed at proving the efficiency of a tunable heterodyne receiver in combustion pollutants remote sensing. For this purpose, we developed the instrument and validated by recording an emission spectrum of SO₂. The SO₂ was present at high temperature in a real combustion system; it was added in the CH₄/air mixture producing a flame.

It appears that the instrument detection limit is a received mid-IR flux of 2×10^{-13} W, which is an excellent result when a lead salt laser is used as LO.

By way of improvement, we gave a panel of semiconductor lasers still in development, which will provide alternative tunable LOs. We gave minimum detectable concentration of several molecules in case of a heterodyne receiver whose detection limit is increased by a factor 100.

Acknowledgements

We wish to thank Yuriy Selivanov from the Lebedev Institute (Moscow) for having provided us the diode laser used in this work.

References

- [1] Hemmerling B, Radi P, Stampanoni-Panariello A, Kouzov A, Kozlov D. Novel non linear optical techniques for diagnostics: laser induced gratings and two colour four wave mixing. *C R Acad Sci Paris* 2001;2(IV):1001–12.
- [2] Gutfleisch M, Shin DI, Dreier T, Danehy PM. Mid-infrared laser-induced grating experiments of C₂H₄ and NH₃ from 0.1–2 Mpa and 300–800 K. *Appl Phys B* 2000;71:673–80.
- [3] Hart RC, Balla RJ, Herring GC. Observation of H₂O in a flame by two-colour laser-induced-grating spectroscopy. *Meas Sci Technol* 1997;8:917–20.
- [4] Cooper CS, Laurendeau NM. Laser-induced fluorescence measurements in lean direct-injection spray flames: technique development and application. *Meas Sci Technol* 2000;11:902–11.
- [5] Clauss W, Fabelinsky VI, Kozlov DM, Smirnov VV, Stelmakh OM, Vereschagin KA. Dual broadband CARS temperature measurements in hydrogen–oxygen atmospheric pressure flames. *Appl Phys B* 2000;70:127–31.
- [6] Hussong J, Stricker W, Bruet X, Joubert P, Bonamy J, Robert D, Michaut X, Gabard T, Berger H. Hydrogen CARS thermometry in H₂–N₂ mixtures at high pressure and medium temperatures: influence of linewidths models. *Appl Phys* 2000;70:447–54.
- [7] Bood J, Bengtsson PE, Alden M. Temperature and concentration measurements in acetylene–nitrogen mixtures in the range 300–600 K using dual-broadband rotational CARS. *Appl Phys B* 2000;70:607–20.
- [8] Werle P. A review of recent advances in semiconductor laser based gas monitors. *Spectrochim Acta* 1998;A54:197–236.
- [9] Mantz AW. A review of spectroscopic applications of tunable semiconductor lasers. *Spectrochim Acta* 1995;A51:2211–36.
- [10] Fried A, Henry B, Wert B, Sewell S, Drummond JR. Laboratory, ground based, and airborne tunable diode laser systems: performance characteristics and application in atmospheric studies. *Appl Phys B* 1998;67:317–30.
- [11] Webster CR, Flesch GJ, Scott DC, Swanson JE, May RD, Woodward WS, Gmachl C, Capasso F, Sivco DL, Baillargeon JN, Hutchinson AL, Cho AY. Quantum cascade laser measurements of stratospheric methane and nitrous oxide. *Appl Opt* 2001;40(3):321–6.
- [12] Browell EV, Ismail S, Grant WB. Differential absorption lidar (DIAL) measurements from air and space. *Appl Phys B* 1998;67:399–410.
- [13] Weibring P, Edner H, Svanberg S, Cecchi G, Pantani L, Ferrara R, Caltabiano T. Monitoring of volcanic sulfur dioxide emissions using differential absorption lidar (DIAL), differential optical absorption spectroscopy (DOAS), and correlation spectroscopy (COSPEC). *Appl Phys B* 1998;67:419–26.
- [14] Fujii T, Fukuchi T, Cao N, Nemoto K, Takeuchi N. Trace atmospheric SO₂ measurement by multiwavelength curve fitting and wavelength optimized dual differential absorption lidar. *Appl Opt* 2002;43(3):524–31.
- [15] Thomasson A, Geffroy S, Frejafon E, Weidauer D, Fabian R, Godet Y, Nominé M, Ménard T, Rairoux P, Moeller D, Wolf JP. LIDAR mapping of ozone-episode dynamics in Paris and intercomparison with spot analysers. *Appl Phys B* 2002;74:453–9.
- [16] <http://tes.jpl.nasa.gov/>
- [17] Menzies RT. Laser heterodyne detection techniques. In: Hinkley ED, editor. *Laser monitoring of the atmosphere*. Berlin: Springer, 1976.

- [18] Beck M, Hofstetter D, Aellen T, Faist J, Oesterle U, Ilegems M, Gini E, Melchior H. Continuous wave operation of a mid-infrared semiconductor laser at room temperature. *Science* 2002;295:301–5.
- [19] Weidmann D, Courtois D. Infrared 7.6 μm lead salt diode laser heterodyne radiometry of water vapor in a CH_4/air premixed flame. *Appl Opt* 2003;42(6):1115–21.
- [20] Tiuri ME. Radio astronomy receivers. *IEEE Trans Antennas Propag* 1964;12(7):930–8.
- [21] Mumma MJ, Kostiuik T, Buhl D, Chin G, Zipoy D. Infrared heterodyne spectroscopy. *Opt Eng* 1982;21(2):313–9.
- [22] Tacke M, Spanger B, Lambrecht A, Norton PR, Böttner H. Infrared double heterostructure diode lasers made by molecular beam epitaxy of PbEuSe . *Appl Phys Lett* 1999;53(23):2260–2.
- [23] Katzberg SJ, Kowitz HR, Rowland CW. Noise effects in an optical heterodyne spectrometer using tunable diode lasers. *Appl Phys Lett* 1981;39(9):688–90.
- [24] Allario F, Katzberg SJ, Larsen JC. Sensitivity studies and laboratory measurements for the heterodyne spectrometer experiment. In: *Heterodyne systems and technology*, NASA CP2138, Williamsburg 1980. p. 221–40.
- [25] Teich MC. Coherent detection in the infrared, in semiconductors and semimetals. In: Williardson RK, Beer AC, editors. *Infrared detectors*, vol. 5. New York: Academic Press, 1970.
- [26] Blaney TG. Signal to noise ratio and other characteristics of heterodyne radiation receivers. *Space Sci Rev* 1975;17:691–702.
- [27] Fink D. Coherent detection signal to noise. *Appl Opt* 1975;14(3):689–90.
- [28] Kostiuik T, Mumma MJ, Abbas MM, Buhl D. Sensitivity of an astronomical infrared heterodyne spectrometer. *Infrared Phys* 1976;16:61–4.
- [29] Rothman LS, Rinsland CP, Goldman A, Massie ST, Edwards DP, Flaud JM, Perrin A, Camy-Peyret C, Dana V, Mandin JY, Schroeder J, McCann A, Gamache RR, Wattson RB, Yoshino K, Chance KV, Jucks KW, Brown LR, Nemtchinov V, Varanasi P. The HITRAN Molecular Spectroscopic Database and HAWKS (HITRAN Atmospheric Workstation): 1996 Edition. *JQSRT* 1998;60:665–710.
- [30] Weidmann D, Courtois D. High quality infrared (8 μm) diode laser source design for high resolution spectroscopy with precise temperature and current control. *Infrared Phys Technol* 2000;41:361–71.
- [31] Weidmann D, Hamdouni A, Courtois D. $\text{CH}_4/\text{air}/\text{SO}_2$ premixed flame spectroscopy with a 7.5 μm diode laser. *Appl Phys B* 2001;73:85–91.
- [32] DeBaker MR, Parvitte B, Thomas X, Zeninari V, Courtois D. Tunable diode laser spectrometer apparatus function. *JQSRT* 1998;59:3–5.
- [33] Bewley WW, Felix CL, Vurgaftman I, Stokes DW, Aifer EH, Olafsen LJ, Meyer JR, Yang MJ, Shanabrook BV, Lee H, Martinelli RU, Sugg AR. High temperature continuous wave 3–6.1 μm W lasers with diamond pressure bond heat sinking. *Appl Phys Lett* 1999;74(8):1075–7.
- [34] Shi Z, Xu G, McCann PJ, Fang XM, Dai N, Felix CL, Bewley WW, Vurgaftman I, Meyer JR. IV–VI compound midinfrared high reflectivity mirrors and vertical cavity surface emitting lasers grown by molecular beam epitaxy. *Appl Phys Lett* 2000;76(25):3688–90.
- [35] Yang RQ, Bruno JD, Bradshaw JL, Pham JT, Wortman DE. Interband cascade lasers: progress and challenges. *Physica E* 2000;7:69–75.
- [36] Beck M, Hofstetter D, Aellen T, Faist J, Oesterle U, Ilegems M, Gini E, Melchior H. Continuous wave operation of a mid-infrared semiconductor laser at room temperature. *Science* 2002;295:301–5.